Measurement of a Doubly Substituted Methane Isotopologue, [superscript 13]CH[subscript 3]D, by Tunable Infrared Laser Direct Absorption Spectroscopy

Measurement of a Doubly-Substituted Methane Isotopologue, $^{13}CH_3D$, by Tunable Infrared Laser Direct Absorption Spectroscopy

Shuhei Ono,[*1], David T. Wang[1], Danielle S. Gruen[1], Barbara Sherwood Lollar[2], Mark S. Zahniser[3], Barry J. McManus[3], David D. Nelson[3]*

[1]Department of Earth, Atmospheric and Planetary Sciences, Massachusetts Institute of Technology, Cambridge, MA. sono@mit.edu

[2]Department of Earth Sciences, University of Toronto, Toronto, ON, Canada

[3]Center for Atmospheric and Environmental Chemistry, Aerodyne Research, Inc., Billerica, Massachusetts, USA

Keywords: Tunable Laser Spectroscopy, Quantum Cascade Laser, Methane, Isotopologue, Clumped Isotope

* Corresponding author, sono@mit.edu

A manuscript prepared for submission to Analytical Chemistry March 18, 2014

5520 words, 7 figures (equivalent to ~1200 words), 2 tables (250 to 400 words)

Abstract

Methane is an important energy resource and significant long-lived greenhouse gas. Carbon and hydrogen isotope ratios have been used to better constrain the sources of methane, but interpretations based on these two parameters alone can often be inconclusive. The precise measurement of a doubly-substituted methane isotopologue, $^{13}CH_3D$, is expected to add a critical new dimension to source signatures by providing the apparent temperature at which methane was formed or thermally equilibrated. We have developed a new method to precisely determine the relative abundance of $^{13}CH_3D$ by using tunable infrared laser direct absorption spectroscopy (TILDAS). The TILDAS instrument houses two continuous wave quantum cascade lasers; one tuned at 8.6 μm to measure $^{13}CH_3D$, $^{12}CH_3D$ and $^{12}CH_4$, and the other at 7.5 μm to measure $^{13}CH_4$. Using an astigmatic Herriott cell with an effective pathlength of 76 m, a precision of 0.2 ‰ (2σ) was achieved for the measurement of $^{13}CH_3D$ abundance in ca. 10 mL STP (i.e., 0.42 mmol) pure methane samples. Smaller quantity samples (ca. 0.5 mL STP) can be measured at lower precision. The accuracy of the $\Delta^{13}CH_3D$ measurement is 0.7‰ (2σ), evaluated by thermally-equilibrating methane with a range of δD values. The precision of ±0.2‰ corresponds to uncertainties of ±7°C at 25°C and ±20°C at 200°C for estimates of apparent equilibrium temperatures. The TILDAS instrument offers a simple and precise method to determine $^{13}CH_3D$ in natural methane samples to distinguish geological and biological sources of methane in the atmosphere, hydrosphere, and lithosphere.

Introduction

Methane is the second most important long-lived greenhouse gas, and an increasingly important energy resource.[1] Abrupt changes in reservoirs and fluxes of methane in the Earth's surface may have been responsible for triggering abrupt climate change in the past[2]. The atmospheric methane level increased through much of the twentieth century, but the growth rate slowed and the concentration appeared to have plateaued between 1999 and 2007, at which point growth resumed.[3] The main drivers for this secular trend have been debated, with explanations ranging from changes in source (e.g., wetlands vs. fossil fuel emissions) and/or sink (oxidation by OH radical) strengths.[3-5]

The majority of environmental methane is of biogenic (originating from microbial methanogenesis) or thermogenic (produced by thermal cracking of higher molecular weight hydrocarbons, kerogen and coal) origin, with contributions from biomass burning and, in certain geologic environments, putative abiotic sources (e.g., serpentinite and deep crustal fluids).[6-8]

Carbon ($^{13}C/^{12}C$) and hydrogen (D/H) isotope ratios of methane and associated short-chain hydrocarbons have been used to elucidate their sources[9,10] but such data alone can often be inconclusive because of significant overlap in isotopic signatures associated with microbial, thermogenic and abiogenic gases. This is because the $^{13}C/^{12}C$ ratio of methane depends on the carbon source (e.g., CO_2, acetate) and its isotopic composition,[11] the isotope effects associated with microbial methanogenesis or thermal cracking, and the effects of secondary processes, such as oxidation and mixing.[12,13] The D/H ratio of methane is also a complex function of reaction pathways, the D/H ratio of environmental water, and the D/H ratio of precursor compounds.[14,15] Therefore, the development of a new constraint, such as an isotopic thermometer, could unlock critical information to constrain the source of methane.

In this study, we report a methane isotope thermometry method based on the measurements of the doubly-substituted ("clumped") methane isotopologue, $^{13}CH_3D$. Following earlier studies of doubly-substituted carbon dioxide ($^{13}C^{16}O^{18}O$),[19] the precise measurements of four or more isotopologues of methane ($^{12}CH_4$, $^{13}CH_4$, $^{12}CH_3D$, and $^{13}CH_3D$) may allow estimation of the temperature at which a sample of methane was formed or thermally equilibrated.[20,21]

Carbon ($^{13}C/^{12}C$) and hydrogen (D/H) isotope ratios of methane have been routinely measured by gas-source isotope-ratio mass spectrometry (IRMS). Conventional IRMS techniques for measuring carbon- and hydrogen-isotope ratios involve combustion or pyrolysis of methane, respectively, and measurement of the isotopologue ratios of the product CO_2 or H_2.[9,22] Direct measurement of $^{13}CH_3D^+$ ion is required, however, for mass-spectrometric determination of $^{13}CH_3D$. This is technically challenging because of the low fractional abundance of $^{13}CH_3D$ (ca. 3 to 8 ppm) and interferences from adduct ($^{13}CH_5^+$) and $^{12}CH_2D_2^+$ ions. Fragment ions (e.g., CH_3^+, CH_2^+) also complicate mass-16 ($^{12}CH_4^+$) and mass-17 ($^{12}CH_3D^+$ and $^{13}CH_4^+$) signals. Resolving these isobars requires the use of double-focusing high resolution gas-source IRMS.[21,23] Stolper et al. (2014)[21] report the first precise measurements of methane clumped isotopologue abundance (combined $^{13}CH_3D$+$^{12}CH_2D_2$) by using medium mass-resolving power (M/ΔM) from 16,000 to 25,000; contributions of adduct ions ($^{13}CH_5^+$ on $^{13}CH_3D^+$, and $^{12}CH_5^+$ on $^{12}CH_3D^+$) were corrected as a function of mass-16 ion current.

In this study, we report the application of tunable infrared laser direct absorption spectroscopy (TILDAS) for the fully-resolved measurement of a clumped isotopologue of methane, $^{13}CH_3D$. TILDAS is a virtually non-destructive technique, and offers a promising approach for precise and direct measurements of methane isotopologues. Bergamaschi et al. (1994)[24] reported

measurements of $^{13}CH_4$ and $^{12}CH_3D$ using a lead salt diode laser tuned in the ~3.3 μm regions (ν_3 band). Precisions of 0.44 and 5.1 ‰ were achieved for $\delta^{13}C$ and δD measurements, respectively (δ values are defined as the deviation of the isotope ratios $^{13}C/^{12}C$ and D/H with respect to reference materials). Recently, a tunable laser spectroscopy instrument with an interband cascade laser tuned at 3.27μm was used for the detection of methane on the Mars *Curiosity* rover mission.[25] Tsuji et al., (2012)[26] reported the first optical measurement of $^{13}CH_3D$ using a difference-frequency-generation laser in the 3.4μm region. Their reported analytical precision of 20‰ (1σ), however, was too large to resolve the thermodynamically-predicted natural range of variation of $^{13}CH_3D$ abundances (ca. 6‰).

The TILDAS instrument used in this study takes advantage of quantum cascade lasers (QCLs) that allow for continuous wave (cw) operation near room temperature, with high power (tens of mW) and narrow linewidths (<0.001 cm-1 ≃ 30 MHz). These lasers access the 8 μm (ν_4) band system of CH_4, where several isolated absorption bands are available. Previously, a TILDAS instrument equipped with a cwQCL achieved a precision of 0.2 to 0.5 ‰ for $^{13}CH_4/^{12}CH_4$ ratios during continuous sampling of ambient air (~1.8 ppm CH_4 mixing ratio).[27,28] This report describes the application of a dual laser TILDAS instrument for the precise measurement of the abundance of $^{13}CH_3D$ in pure samples of methane. We report here the selection and characterization of absorption lines, the construction of a dual-inlet sample introduction system, the results of calibration and performance testing, and some preliminary data obtained by the TILDAS instrument.

Principle of Methane Isotopologue Thermometry

The goal of this study is to develop methane isotopologue thermometry based on the following isotope exchange reaction among four isotopologues of methane:

$$^{13}CH_4 + {}^{12}CH_3D \leftrightarrow {}^{13}CH_3D + {}^{12}CH_4 \quad (1)$$

The equilibrium constant (K) for this reaction is a function of temperature:

$$K(T) = \frac{[^{13}CH_3D][^{12}CH_4]}{[^{12}CH_3D][^{13}CH_4]} \quad (2)$$

where brackets represent the abundance (e.g., mixing ratio) of each methane isotopologue. The equilibrium constant approaches unity at very high temperatures (>1,000K), and referred to as a stochastic distribution. At lower temperatures, however, statistical mechanics theory predicts that the equilibrium for (1) lies slightly toward the right ($K \simeq 1.006$ at room temperature, *see* Supporting Information, SI).

Defining $\Delta^{13}CH_3D$ as the natural logarithm for equation (2) gives:

$$\Delta^{13}CH_3D = \ln(K) = \ln\frac{[^{13}CH_3D]}{[^{12}CH_3D]} - \ln\frac{[^{13}CH_4]}{[^{12}CH_4]} \quad (3)$$

The definition of $\Delta^{13}CH_3D$ in equation (3) yields values that are practically identical to those calculated using the definition used by Stolper et al. (2014)[21] (i.e., the deviation from stochastic distribution. *see* SI).

In this study, we use conventional delta notation to express ratios of isotopologue abundance in a sample with respect to those of a reference. For example,

$$\delta^{13}CH_3D = \frac{([^{13}CH_3D]/[^{12}CH_4])_{sample}}{([^{13}CH_3D]/[^{12}CH_4])_{reference}} - 1 \quad (4)$$

For practical purposes (under expected ranges of multiply-substituted isotopologue abundance for natural samples), $\delta^{13}CH_4$ is identical to $\delta^{13}C$ and $\delta^{12}CH_3D$ is identical to δD.

Experimental Section

Synthesis of Methane Isotopologues

Methane isotopologues, $^{13}CH_3D$, CH_3D (natural abundance $^{13}C/^{12}C$), and CH_4 (D-depleted) were synthesized for spectral characterization and to produce a series of working standard gases. The clumped methane isotopologue, $^{13}CH_3D$, was synthesized by the Grignard reaction from ^{13}C-iodomethane and D_2O. Similarly, CH_3D (with natural-abundance ^{13}C) was synthesized from iodomethane and D_2O. D-depleted methane was synthesized from aluminum carbide (Al_4C_3, natural C isotope abundance) and D-depleted water (D content 2-3 ppm) (*See* SI for detailed description of synthesis procedures).

Selection of Absorption Lines

Among several possible methane infrared band systems, a spectral region around 8.6 μm was selected. Tsuji et al. (2012)[26] reported measurements of $^{13}CH_3D$ in the 3.4 μm region. However, they used dry ice to cool the absorption cell in order to reduce hot bands and high-J fundamental bands from major isotopologues. The absorption band system at 8.6 μm is highly advantageous because of less interference from hot bands in this region, and the availability of line parameters in the HITRAN database.[29] A single deuterium substitution in CH_4 reduces its symmetry from T_d to C_{3v}. As a result, the triply degenerate C-H bending mode of CH_4 centered at 1300 cm^{-1} splits into C-D bending of $^{13}CH_3D$ and $^{12}CH_3D$. The resultant C-D bending mode is about 150 cm^{-1} lower in frequency than the C-H bending vibration. This relatively large frequency shift by deuterium substitution allows us to measure $^{13}CH_3D$ and $^{12}CH_3D$ lines that are free from strong lines originating from the much more abundant $^{12}CH_4$ (Figure 1).

The spectral window between 1168.885 and 1168.995 cm^{-1} was chosen to access three isotopologue lines of $^{13}CH_3D$, $^{12}CH_3D$ and $^{12}CH_4$ (Figure 1 and 2). These three lines are virtually-free from spectral interference, and have relatively low lower-state energies (59, 470, and 861 cm^{-1} for $^{13}CH_3D$, $^{12}CH_3D$, and $^{12}CH_4$, respectively), such that temperature-dependence is expected to be minor (<0.15‰/10mK, Table 1). The absorption line for $^{13}CH_4$ was measured in a spectral window between 1330.94 and 1331.02 cm^{-1} (Figure 2). This line was selected because the line strength is comparable to other isotopologues (~10^{-24} cm/molecule) such that the line does not saturate.

TILDAS Spectrometer

The TILDAS instrument used in this study is based on direct absorption using the astigmatic multipass Herriott cell developed by Aerodyne Research.[30] The instrument houses two continuous wave quantum cascade lasers (QCLs) (Alpes Laser, Switzerland). The first laser (L1) is tuned to $^{12}CH_4$ and $^{13}CH_4$ line at 1331 cm^{-1}, and the second (L2) is tuned to $^{12}CH_3D$, $^{12}CH_4$ and $^{13}CH_3D$ absorption lines at 1169 cm^{-1}. The lasers are housed in hermetically-sealed boxes, and their temperatures are controlled by Peltier elements at 2.6 and -1.8 °C for L1 and L2, respectively. The supply voltages to the QCLs are ramped at a rate of 1.4 kHz to scan the laser frequency across 300 channels for L1 and 600 channels for L2 with additional 100 channels for laser shut off to measure zero-light level. The laser frequency tuning rates are measured by a germanium etalon, and fitted with a cubic spline function. The absorption cell is an astigmatic multipass cell with 76 m effective pathlength with 32 cm base length, and an approximately 500 mL cell volume. The detector is a thermoelectrically-cooled photoconductive (HgCdTe) detector. A spectral baseline was determined by filling the absorption cell with nitrogen (UHP

grade) at a pressure 50% higher than the CH_4 sample pressure to compensate for the higher index of refraction of CH_4 compared to N_2. The cell temperature was monitored by a 30 kΩ thermistor, and the pressure was measured by a capacitance manometer (10 torr full scale, MKS, Andover, MA).

Significant efforts were made towards dampening temperature fluctuations to minimize the temperature dependence of line strengths as well as to improve the stability of the optical train. The optic housing is thermally insulated and temperature regulated at 295 K with air-liquid heat exchangers and cooling water supplied by a recirculating chiller. The temperature stability of the absorption cell is typically within 10 to 20 mK despite up to 2 K fluctuations in the laboratory air temperature. The number density of each isotopologue is estimated at a rate of 1 Hz by a least-square spectral fit assuming Voigt line profile, taking into account the temperature and pressure inside the absorption cell (Figure 2).

Gas Inlet System

A gas inlet system was constructed to introduce sample CH_4 at a controlled pressure (Figure 3). TILDAS is commonly used to measure samples in a flow-through system for continuous measurements. In this study, however, the CH_4 sample was introduced into a pre-evacuated absorption cell by expansion and then isolated for absorption measurements. The leak rate of the absorption cell is 0.01 torr/hour, which is negligible for the duration of analysis for a pair of sample and reference measurement (ca. 12 minutes; Figure S-1).

The inlet system is constructed with twenty pneumatically-operated high-purity diaphragm or bellow-sealed valves (DP or BK series, Swagelok, OH), a mass flow controller (Aalborg, NY), two capacitance manometers (250 torr full scale, MKS, Andover, MA), two adjustable bellows

189 volumes, and a scroll pump (SH-110, Agilent). These components are controlled via custom-
190 built software routines implemented in LabVIEW (National Instruments). Sample CH_4 (5 to 10
191 mL STP) is introduced into the two separate adjustable bellows volumes (Metal Flex, Newport,
192 VT). The internal volume of the bellows can be adjusted between 50 mL and 490 mL using a
193 linear actuator, allowing the CH_4 pressure to be controlled to within ±0.1 torr. A portion of
194 sample methane can be introduced into the laser cell by expanding it into the expansion volume
195 V1 (ca. 10 mL) (Figure 3).
196 Each measurement cycle (ca. 12 min) consists of the following sequence of events (Figure S-
197 1). First, baseline measurements are taken, during which UHP nitrogen is supplied from a mass
198 flow controller and flushed through the absorption cell. This is followed by pumping down the
199 cell using a turbomolecular pump. Sample CH_4 is introduced to the expansion volume (V1), and
200 then to the absorption cell at a pressure of 0.80 ± 0.006 (2σ) torr (0.53 mL STP or 22 μmol).
201 After measurement of the sample CH_4, the cell is flushed with nitrogen, and evacuated. Then,
202 reference CH_4 is introduced into the absorption cell. The measurement cycles (baseline, sample,
203 reference) are repeated 5 to 10 times (time per cycle is 12 minutes). The bellows are compressed
204 after each measurement cycle to maintain the same sample pressure. The typical standard
205 deviation on $\Delta^{13}CH_3D$ for each cycle is 0.6 ‰ (2σ). Thus, the standard error of the mean
206 approaches 0.2 to 0.3 ‰ (2SEM) after 5 to 10 measurement cycles (Table S-1).

207 # Results

208 ## Line Parameters and Spectrum Analysis

209 HITRAN line parameters for measured absorption lines are listed in Table 1. All target
210 isotopologue lines were found at expected transition frequencies (Figure 2). According to the

HITRAN database, the target $^{13}CH_3D$ line (ν_6 $A_1(4,4) \leftarrow A_2(3,3)$ and $A_2(4,4) \leftarrow A_1(3,3)$) is split by 0.002 cm^{-1}. However, we found that the best spectral fit was obtained by assuming no splitting, consistent with recent spectroscopy measurements.[31] A spectrum was also taken with synthesized $^{13}CH_3D$ at a cell pressure below 0.01 torr (estimated to be ca. 0.6 mtorr from the absorption spectrum). The TILDAS spectrum showed a line shape corresponding to a single Doppler line, suggesting that these two lines are nearly degenerate (Figure S-2).

Measured spectra were fit to a Voigt profile, from which the number density of each isotopologue was estimated. The Voigt profile is a convolution of Gaussian and Lorentzian functions, which arise from Doppler and pressure line broadenings, respectively. TILDAS spectra were taken at CH_4 pressures between 0.4 and 2.1 torr CH_4, in order to characterize broadening line widths at different pressures. Gaussian and Lorentzian line widths were derived from a least square fit applied for each pressure (Figure S-3). From this analysis, line widths were parameterized as linear functions of pressure[32,33]:

$$\Gamma_G = \Gamma_D (1+\gamma_{Dicke}) \times pCH_4 \quad (5)$$

$$\Gamma_L = \gamma_P \times pCH_4 \quad (6)$$

where Γ_G and Γ_L are Gaussian and Lorentzian line widths, respectively, and Γ_D is the Doppler line width without Dicke narrowing contribution. The terms, γ_{Dicke} and γ_P, account for the Dicke narrowing and pressure broadening effects, respectively. At the CH_4 pressure used for measurements (ca. 0.8 torr), the Voigt line width is largely due to Doppler broadening (1.8×10^{-3} cm^{-1}, HWHM) with minor contributions from pressure broadening (10^{-4} cm^{-1}) for the main $^{12}CH_4$ line. The laser line width was estimated to be between 1×10^{-4} and 3×10^{-4} cm^{-1}. Using the fit parameters in Table 1, the typical fit residual is less than ±0.02 % across measured spectral regions (Figure 2). The derived pressure broadening factors (γ_P) are higher than HITRAN

values, part of which may be due to underestimated laser line widths or due to uncertainty in laser tuning rates.

Instrument Stability and Measurement Cycles

To test the stability of the instrument, number densities of CH_4 isotopologues were monitored continuously for over 6 hours at a cell CH_4 pressure of 0.8 torr. Allan variance analysis of the data indicates one second Allan deviations of 0.30, 0.25 and 1.3‰ for $\delta^{13}CH_4$, $\delta^{12}CH_3D$, and $\delta^{13}CH_3D$, respectively (Figure 4). White noise dominates the Allan variance up to 120 seconds integration time but system drift becomes significant over timespans longer than 1000 seconds. Ultimate precisions, down to 0.03, 0.04, and 0.2‰, for $\delta^{13}CH_4$, $\delta^{12}CH_3D$, and $\delta^{13}CH_3D$, respectively, can be approached by 120 seconds signal averaging. This analysis indicates the optimum measurement sequence to be longer than 120 seconds signal integration time but less than 1000 seconds (16.6 min) for sample versus reference measurement cycles. Measurement cycle for samples was designed based on the Allan variance analysis (Figure S-1).

Heated Methane Calibration

Standard reference materials with known $^{13}CH_3D$ abundances do not yet exist. Therefore, in order to calibrate the $^{13}CH_3D$ isotopologue scale for TILDAS, a series of experiments were carried out to produce CH_4 isotopologues by thermal equilibration (i.e., reaction 1) using a conventional flame-seal tube technique.[21,37]

A series of methane isotopologue mixtures were produced by the addition of pure isotopologues to natural isotopologue abundance methane (AL1 and AL2). These mixtures include one with $^{13}CH_3D$ spike ($\Delta^{13}CH_3D$ = 36.8 ‰, AL2-D3), and four (AL1-D2, AL1-D3,

AL2-D4, and AL1-D5) with a range of δD values from -628.6 to 273.3 ‰ (Table S-1). Aliquots of these methane mixtures (ca. 8 to 10 mL STP) were condensed in quartz or pyrex tubes containing silica gel and platinum catalyst (Platinum on alumina, Sigma Aldrich) at -196°C. Prior to loading, the silica gel and platinum catalysts were baked at 300°C under vacuum for 1 hour to dehydrate, and then heated by a torch to activate the platinum catalyst (PtO_2 decomposes to Pt above 400 °C under vacuum[38]). These tubes were flame-sealed and heated in an oven at temperatures between 200 and 400 °C (± 4 °C) for days to weeks (Table S-1).

Time Series Experiment

As a proof of concept, non-equilibrium isotopologue abundance methane ($\Delta^{13}CH_3D$ of +36.9 ‰, AL2-D3, Table S-1) was produced by adding synthesized $^{13}CH_3D$ to natural-abundance methane cylinder gas (Table S-1). A series of flame sealed tubes were prepared with the isotopologue labeled methane and heated at 200°C. The tubes were quenched between 5 and 19 days, and the resulting methane was distilled at -196°C and analyzed by TILDAS. The large positive $\Delta^{13}CH_3D$ signal disappeared after 8 days (at *e*-folding time of 0.52 day), and reached a value of 0.08±0.15 ‰ after 19 days (Figure 5). Ideally, the isotope exchange reaction does not change the bulk isotopologue ratios (amount of the $^{13}CH_3D$ spike is minor compared to $^{13}CH_4$ and $^{12}CH_3D$). As expected, the value of $\delta^{13}C$ stayed nearly constant (+0.11±0.03 ‰) but the δD value decreased by 21 to 23 ‰, suggesting that some chemical reaction did occur (Table S-1). This is confirmed by gas chromatography analysis, which indicated the presence of H_2 and CO_2 in the heated methane samples. Hydrogen was likely formed from decomposition of methane to H_2 and graphite; the oxygen in CO_2 may have come from PtO_2 film or residual water on silica gel or Pt catalyst. The rapid disappearance of the $\Delta^{13}CH_3D$ signal indicates that the isotope

exchange reaction, however, occurred at a faster rate than the decomposition, consistent with observations by Stolper et al. (2014).[21]

δD Bracketing Experiment

The δD values of natural methane samples can vary from -500 to -50‰.[10] One of the major challenges for accurate measurements of $\Delta^{13}CH_3D$ value is defining the linearity of the instrument over a wide range of δD values. For example, if there is a very weak $^{12}CH_4$ absorption line under $^{12}CH_3D$ that is not registered in the HITRAN database, the δD isotope scale will be compressed (e.g., δD of -500‰ might be measured as -499‰). In order to test the linearity of the instrument, isotopologue bracketing experiments were carried out following Stolper et al. (2014)[21] using a series of methane gases with δD values ranging from -629 to 263‰ (Figure 6; Table S-1). Aliquots of these methane isotopologue mixtures were flame-sealed in quartz tubes and heated at 400°C for one day or longer in the presence of Pt catalyst.

The $\Delta^{13}CH_3D$ values of these gases ranged from -1.60 to 0.11 ‰ after heating (Figure 6B). The values of $\Delta^{13}CH_3D$ correlate with δD values with a least-squares fit of $\Delta^{13}CH_3D = -0.0027 \cdot \delta D - 0.61$ (Figure 6B). From this correlation, a scale compression factor of 0.2% was estimated (the difference between 0.0027 and 0.0020 is because the working standard, AL1, has a non-zero δD value with respect to SMOW), and used to correct all the data. This suggests that there could be a weak absorption line beneath $^{12}CH_3D$. A weak line with line strength ~ 2×10^{-27} cm/molecule (i.e., 0.2 % of $^{12}CH_3D$ line strength) would only produce a 0.01% signal in a fit residual and would be difficult to detect (Figure 2). This "scale expansion correction" was applied such that raw δD values (δD value with respect to reference gas AL1) were multiplied by 1.002 to obtain the corrected δD values[39] (*see* SI). The corrected average $\Delta^{13}CH_3D$ value is -

0.88±0.66‰ (2σ) (Figure 6C), which is 0.3 ‰ higher than that measured for samples of the laboratory working reference gas (AL1) that were heated to the same temperature (400°C). The accuracy for $\Delta^{13}CH_3D$ value is estimated to be 0.66‰ (2σ), and is limited by uncertainty in measurements on heated methane samples used for the calibration.

It is unclear if this apparent bias of 0.3‰ is due to spectroscopic artifacts from TILDAS, experimental procedures for thermal equilibrium experiments, or sample preparation steps. For experiments with highly D-enriched (AL1-D3) or depleted (AL2-D4) starting methane, the δD value changed from 273‰ down to 88‰ (AL1-D3) or from -629 to -379‰ (AL2-D4), clearly indicating some chemical reactions occurred in addition to the isotope exchange. Experiments run at 400°C yielded more H_2 and H_2O/CO_2 (both ca. 2 % of initial CH_4) compared to those run at 200°C experiments that yielded ca. 1% CO_2/H_2O of CH_4 without H_2, as estimated from pressure during sample handling. These chemical reactions (e.g., decomposition of CH_4 to H_2 and graphite) may be responsible for the bias for $\Delta^{13}CH_3D$. Stolper et al. (2014)[21] reported that sample introduction fractionated their $\Delta^{13}CH_3D$ value by 0.49‰ when molecular sieve adsorbent was not heated to 150 °C during desorption. A similar isotope fractionation due to incomplete desorption from silica gel may also explain some scatter in the data. Potential isotope fractionation during sample handling procedures is currently under investigation.

Methane isotopologue temperature calibration

A series of experiments was carried out to equilibrate reference methane (AL1) at temperatures between 200 and 400 °C, and to compare with theoretical estimates (Figure 7, Table S-1). Methane equilibrated at 200, 300 and 400°C yielded $\Delta^{13}CH_3D$ (with respect to unheated AL1) values of 0.14±0.15, -0.71±0.14, and -1.23±0.39 ‰ (2SEM), indicating that reference gas AL1

(commercial UHP grade methane) has $\Delta^{13}CH_3D$ value of +2.29±0.15 ‰ with respect to a stochastic $^{13}CH_3D$ abundance. Thus, our working standard gas, AL1, has an apparent $^{13}CH_3D$ isotopic temperature of 212±10°C.

Methane Isotopologue temperatures of cylinder gas and natural gas

Methane from commercially-available cylinders of high-purity methane (AL1, AS1, and AS2) and from a natural gas tap at MIT ("house gas") were measured using TILDAS. Results of these measurements are shown in Table 2. The three cylinders of methane and the house natural gas yield $\delta^{13}C$ values ranging from -33.6 to -42.4‰ (with respect to VPDB), δD values between -127 and -161‰ (with respect to VSMOW), and $\Delta^{13}CH_3D$ values of 2.3 to 3.0‰ (with respect to the stochastic distribution). The values for $\delta^{13}C$ and δD are within the typical range for methane in natural gas from thermogenic sources.[10] The derived $\Delta^{13}CH_3D$ temperature ranges from 151 to 212°C, consistent with the temperature range within which thermogenic methane is thought to be generated (the "gas window"). Repeated measurements on two in-house cylinder gasses, AS1 and AS2, with respect to a working standard gas (AL1) yield precisions (2σ reproducibility) for $\Delta^{13}CH_3D$ of 0.17 ‰ (n=7) and 0.08 ‰ (n=5), respectively (Table 2).

Conclusions

We have developed a method to precisely determine the relative abundance of a doubly-isotope substituted isotopologue of methane, $^{13}CH_3D$, by measuring the mid-infrared absorption spectrum at 8.6 μm using a TILDAS instrument. A sample gas inlet system was developed for the TILDAS, with which a precision of 0.2‰ (2σ) and an accuracy of 0.7 ‰ (2σ) were achieved for the measurement of $\Delta^{13}CH_3D$ values. Current accuracy is limited by the calibration of

$\Delta^{13}CH_3D$ values against a series of thermally-isotopologue-equilibrated methane samples with a range of δD (and $\delta^{13}C$) values. Future studies will include the development of a robust heating and sample transfer protocol as well as further analysis of spectral features including a potential interfering absorption line beneath the $^{12}CH_3D$ line. Large quantities of sample (ca. 10 mL STP or 420 μmol methane) were used in this study, although samples as small as 0.5 mL STP (=21μmol) can be analyzed at precisions of ±0.6‰ (2σ). Commercially-available cylinders of high-purity methane and natural gas from an in-house tap have $^{13}CH_3D$ temperatures between 150 and 210 °C, consistent with their inferred thermogenic origin. TILDAS instruments are compact, consume little power compared to high-resolution mass-spectrometers,[21] and offer a simple and fully resolved measurement of the doubly substituted methane isotopologue, $^{13}CH_3D$, at natural-abundance levels. The excellent precision attained for $^{13}CH_4$, and for $^{12}CH_3D$ of 0.04‰ by the TILDAS instrument opens up the possibility to apply this technique to high precision analysis of other multiply substituted isotopologues and multiple isotope systems (e.g., $^{43}C^{16}O^{18}O$, $^{12}C^{16}O^{17}O$, $^{14}N^{15}N^{18}O$, $^{33}SO_2$, and $^{36}SO_2$).

Acknowledgments

This work was supported by NSF-EAR 1250394 to S.O., and NSF-AGS 0959280 to S.O., M.Z., B.M., and D.N. Additional support was provided by DOE DE-SC0004575 for M.Z., B.M., and D.N. Funding from Deep Carbon Observatory enabled the acquisition of QCLs and construction of the sample inlet system. Cross-calibration of GC-IRMS results at University of Toronto were funded by the Deep Carbon Observatory and the Natural Sciences and Engineering Research Council of Canada. D.T.W. was supported by an NDSEG Fellowship. D.S.G. acknowledges the Neil and Anna Rasmussen Foundation fund and the Grayce B. Kerr

Fellowship. The authors thank Bill Olszewski, Georges Lacrampe-Couloume, and Stanley Huang for technical assistance, Christopher Glein for suggesting the use of aluminum carbide, Eliza Harris, Craig Schffries, and Robert Hazen for helpful discussions, and two anonymous reviewers for constructive comments.

Supporting Information Available. Additional information as noted in text. This information is available free of charge via the Internet at http://pubs.acs.org/.

References

(1) Brandt, A.; Heath, G.; Kort, E.; O'Sullivan, F.; Pétron, G.; Jordaan, S.; Tans, P.; Wilcox, J.; Gopstein, A.; Arent, D. *Science* **2014**, *343*, 733-735.

(2) Dickens, G. R.; O'Neil, J. R. *Paleoceanography* **1995**, *10*, 965--971.

(3) Rigby, M.; Prinn, R. G.; Fraser, P. J.; Simmonds, P. G.; Langenfelds, R. L.; Huang, J.; Cunnold, D. M.; Steele, L. P.; Krummel, P. B.; Weiss, R. F.; O'Doherty, S.; Salameh, P. K.; Wang, H. J.; Harth, C. M.; M\ hle, J.; Porter, L. W. *Geophysical Research Letters* **2008**, *35*, L22805.

(4) Aydin, M.; Verhulst, K. R.; Saltzman, E. S.; Battle, M. O.; Montzka, S. a.; Blake, D. R.; Tang, Q.; Prather, M. J. *Nature* **2011**, *476*, 198--201.

(5) Kai, F. M.; Tyler, S. C.; Randerson, J. T.; Blake, D. R. *Nature* **2011**, *476*, 194--197.

(6) Sherwood Lollar, B.; Westgate, T. D.; Ward, J. A.; Slater, G. F.; Lacrampe-Couloume, G. *Nature* **2002**, *416*, 522-524.

(7) Proskurowski, G.; Lilley, M. D.; Seewald, J. S.; Früh-Green, G. L.; Olson, E. J.; Lupton, J. E.; Sylva, S. P.; Kelley, D. S. *Science* **2008**, *319*, 604--607.

(8) Etiope, G.; Sherwood Lollar, B. *Reviews of Geophysics* **2013**, *51*, 276-299.

(9) Quay, P.; Stutsman, J.; Wilbur, D.; Dlugokencky, E.; Brown, T. *Global biogeochemical cycles* **1999**, *13*, 445--461.

(10) Whiticar, M. J. *Chemical Geology* **1999**, *161*, 291--314.

(11) Pohlman, J. W.; Kaneko, M.; Heuer, V. B.; Coffin, R. B.; Whiticar, M. *Earth and Planetary Science Letters* **2009**, *287*, 504--512.

(12) Botz, R.; Pokojski, H. D.; Schmitt, M.; Thomm, M. *Organic Geochemistry* **1996**, *25*, 255--262.

(13) Conrad, R. *Organic Geochemistry* **2005**, *36*, 739--752.

(14) Valentine, D. L.; Blanton, D. C.; Reeburgh, W. S. *Archives of Microbiology* **2000**, *174*, 415--421.

(15) Whiticar, M. J.; Faber, E.; Schoell, M. *Geochimica et Cosmochimica Acta* **1986**, *50*, 693--709.

(16) McCollom, T. M.; Lollar, B. S.; Lacrampe-Couloume, G.; Seewald, J. S. *Geochimica et Cosmochimica Acta* **2010**, *74*, 2717-2740.

(17) Taran, Y.; Kliger, G.; Cienfuegos, E.; Shuykin, A. *Geochimica et Cosmochimica Acta* **2010**, *74*, 6112-6125.

(18) Takai, K.; Nakamura, K.; Toki, T.; Tsunogai, U.; Miyazaki, M.; Miyazaki, J.; Hirayama, H.; Nakagawa, S.; Nunoura, T.; Horikoshi, K. *Proceedings of the National Academy of Sciences of the United States of America* **2008**, *105*, 10949--10954.

(19) Eiler, J. M.; Schauble, E. *Geochimica et Cosmochimica Acta* **2004**, *68*, 4767-4777.

(20) Ma, Q.; Wu, S.; Tang, Y. *Geochimica et Cosmochimica Acta* **2008**, *72*, 5446--5456.

(21) Stolper, D.; Sessions, A.; Ferreira, A.; Santos Neto, E.; Schimmelmann, A.; Shusta, S.; Valentine, D.; Eiler, J. *Geochimica et Cosmochimica Acta* **2014**, *126*, 169--191.

(22) Stevens, C. M.; Rust, F. E. *Journal of Geophysical Research* **1982**, *87*, 4879--4882.

(23) Eiler, J. M.; Clog, M.; Magyar, P.; Piasecki, A.; Sessions, A.; Stolper, D.; Deerberg, M.; Schlueter, H. J.; Schwieters, J. *International Journal of Mass Spectrometry* **2013**, *335*, 45-56.

(24) Bergamaschi, P.; Schupp, M.; Harris, G. W. *Applied optics* **1994**, *33*, 7704--7716.

(25) Webster, C. R.; Mahaffy, P. R. *Planetary and Space Science* **2011**, *59*, 271--283.

(26) Tsuji, K.; Teshima, H.; Sasada, H.; Yoshida, N. *Spectrochimica Acta Part A: Molecular and Biomolecular Spectroscopy* **2012**, *98*, 43--46.

(27) Zahniser, M. S.; Nelson, D. D.; McManus, J. B.; Herndon, S. C.; Wood, E. C.; Shorter, J. H.; Lee, B. H.; Santoni, G. W.; Jimenez, R.; Daube, B. C.; Park, S.; Kort, E. A.; Wofsy, S. C. *Proceedings of SPIE* **2009**, *7222*, 72220H.
(28) Santoni, G. W.; Lee, B. H.; Goodrich, J. P.; Varner, R. K.; Crill, P. M.; McManus, J. B.; Nelson, D.; Zahniser, M. S.; Wofsy, S. C. *Journal of Geophysical Research* **2012**, *117*, D10301.
(29) Rothman, L. S.; Gordon, I. E.; Barbe, A.; Benner, D. C.; Bernath, P. E.; Birk, M.; Boudon, V.; Brown, L. R.; Campargue, A.; Champion, J. P.; Chance, K.; Coudert, L. H.; Dana, V.; Devi, V. M.; Fally, S.; Flaud, J. M.; Gamache, R. R.; Goldman, A.; Jacquemart, D.; Kleiner, I.; Lacome, N.; Lafferty, W. J.; Mandin, J. Y.; Massie, S. T.; Mikhailenko, S. N.; Miller, C. E.; Moazzen-Ahmadi, N.; Naumenko, O. V.; Nikitin, A. V.; Orphal, J.; Perevalov, V. I.; Perrin, A.; Predoi-Cross, A.; Rinsland, C. P.; Rotger, M.; Simeckova, M.; Smith, M. A. H.; Sung, K.; Tashkun, S. A.; Tennyson, J.; Toth, R. A.; Vandaele, A. C.; Vander Auwera, J. *J. Quant. Spectrosc. Radiat. Transf.* **2009**, *110*, 533-572.
(30) McManus, J. B.; Kebabian, P. L.; Zahniser, M. S. *Applied Optics* **1995**, *34*, 3336--3348.
(31) Drouin, B. J.; Yu, S.; Pearson, J. C.; Müller, H. S. P. *Journal of Quantitative Spectroscopy and Radiative Transfer* **2009**, *110*, 2077-2081.
(32) Rao, D. R.; Oka, T. *J. Mol. Spectrosc.* **1987**, *122*, 16-27.
(33) Harris, E.; Nelson, D. D.; Olszewski, W.; Zahniser, M.; Potter, K. E.; McManus, B. J.; Whitehill, A.; Prinn, R. G.; Ono, S. *Analytical Chemistry* **2013**, *86*, 1726-1734.
(34) Huntington, K. W.; Eiler, J. M.; Affek, H. P.; Guo, W.; Bonifacie, M.; Yeung, L. Y.; Thiagarajan, N.; Passey, B.; Tripati, A.; Da\ ron, M.; Came, R. *Journal of mass spectrometry : JMS* **2009**, *44*, 1318--1329.
(35) Barkan, E.; Luz, B. *Rapid Communications in Mass Spectrometry* **2005**, *19*, 3737-3742.
(36) Ono, S.; Wing, B.; Johnston, D.; Farquhar, J.; Rumble, D. *Geochimica et Cosmochimica Acta* **2006**, *70*, 2238--2252.
(37) Horita, J. *Geochimica et Cosmochimica Acta* **2001**, *65*, 1907--1919.
(38) Saliba, N. a.; Tsai, Y. L.; Panja, C.; Koel, B. E. *Surface Science* **1999**, *419*, 79--88.
(39) Ono, S.; Wing, B.; Rumble, D.; Farquhar, J. *Chemical Geology* **2006**, *225*, 30-39.

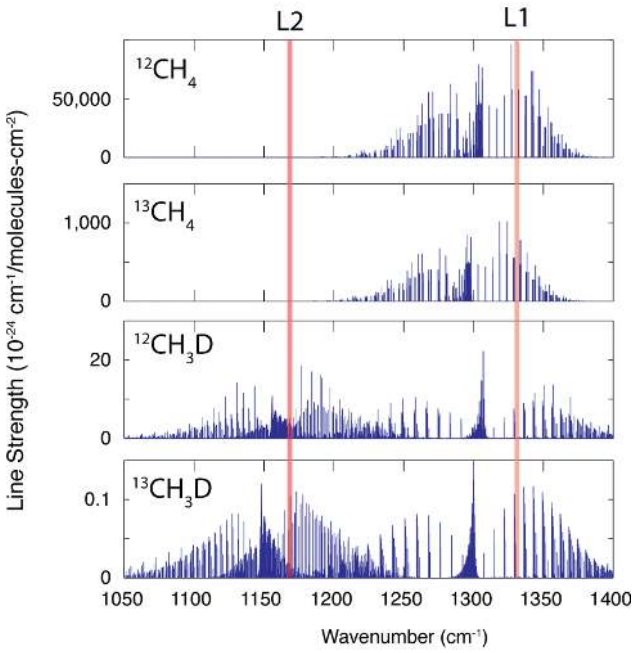

Figure 1. Absorption line positions and strength for four major isotopologues of methane from HITRAN database. Shaded area indicates the spectral windows accessed by two QCL lasers (L1 and L2).

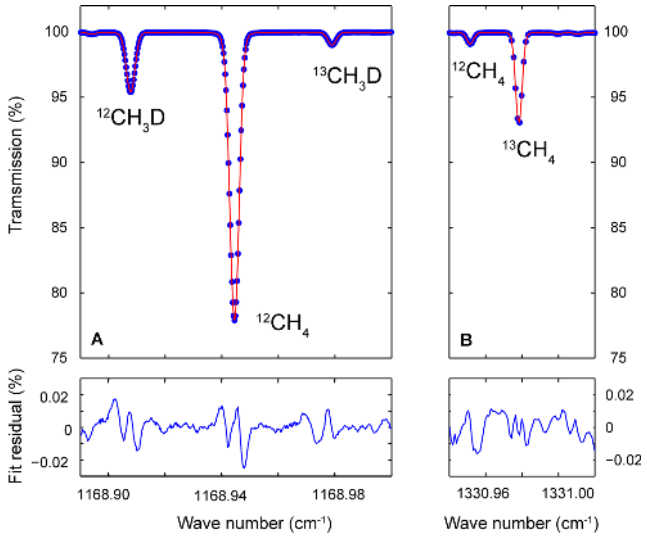

Figure 2. TILDAS Spectrum and fit residual. Left panel (A) is for L2 and right (B) is for L1. Absorption cell is filled with 0.8 torr methane. Blue points are measurements and red lines are spectral fit.

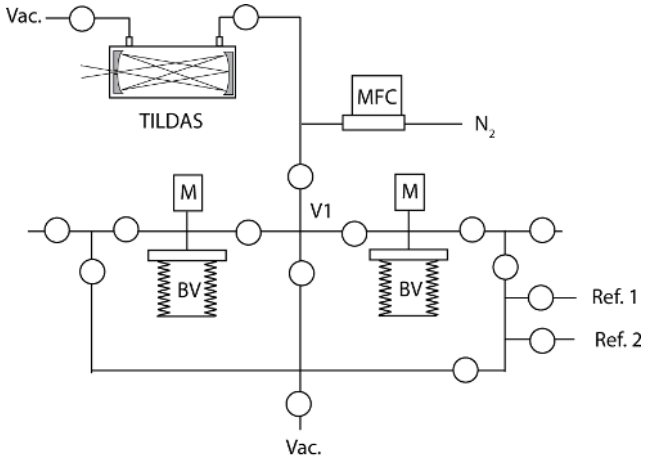

Figure 3. Sample Inlet System constructed for TILDAS instrument. Open Circles are high purity vacuum valves, M: pressure manometer, BV: adjustable bellow volume. MFC: mass flow controller.

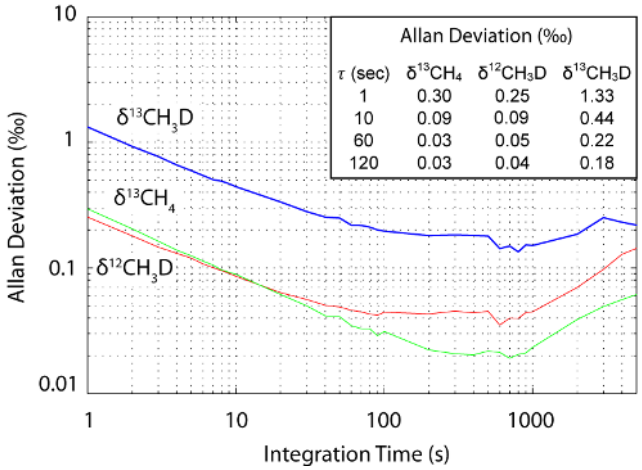

Figure 4. Allan deviation plot for 0.8 torr CH_4 in the laser cell.

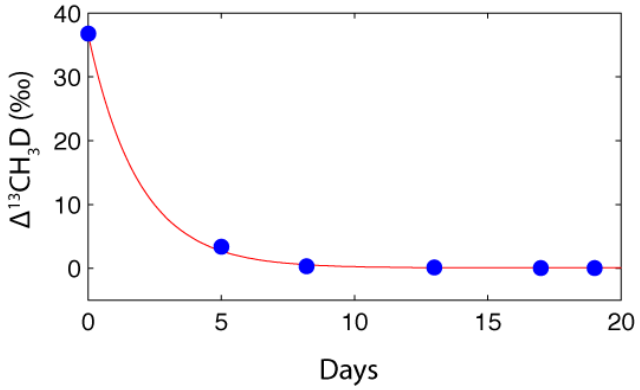

Figure 5. Result of time-series experiment, showing the change of $\Delta^{13}CH_3D$ values for $^{13}CH_3D$ spiked methane (AL2-D3) that is thermally processed at 200°C (Table S-1). Line is a model fit assuming first order kinetics with *e*-folding time of 0.52 days.

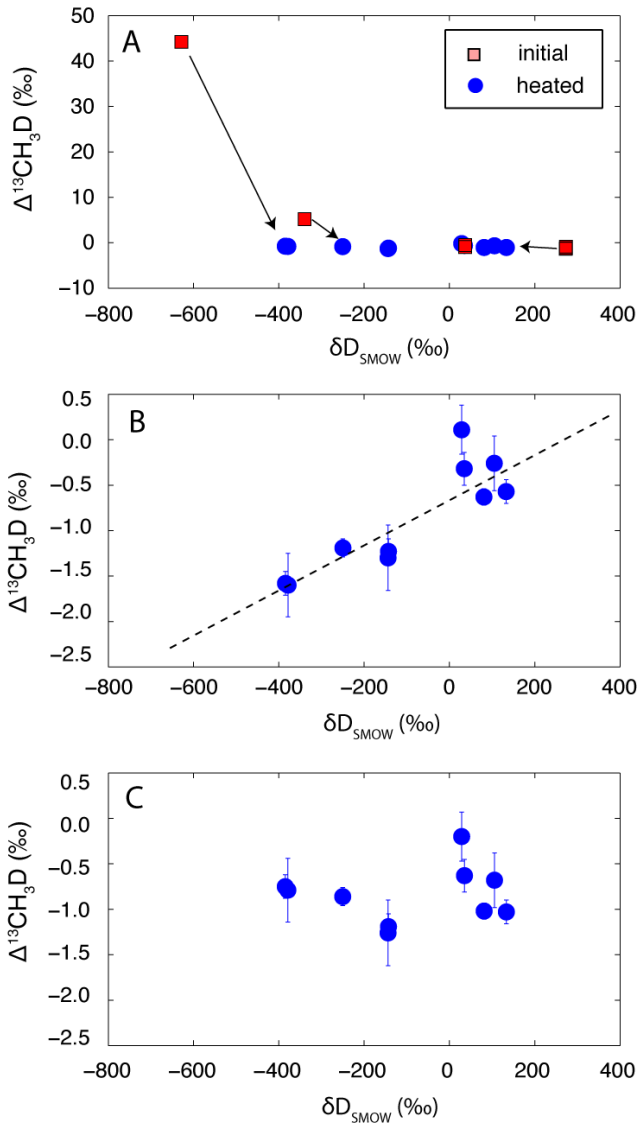

498

499 **Figure 6.** Result of δD bracketing experiments. A) $\Delta^{13}CH_3D$ and δD values for initial methane
500 (square) and heated (circle) methane at 400°C. B) raw results without δD scale correction.
501 Dashed line is a least square fit ($\Delta^{13}CH_3D$ = -0.0027×δD -0.61 ‰). C) after δD scale expansion
502 correction of 1.002. The average $\Delta^{13}CH_3D$ value is -0.84±0.33 ‰ (1σ). *See* Supporting
503 Information for the definition and normalization of δD values.

504

505
506
507
508
509
510

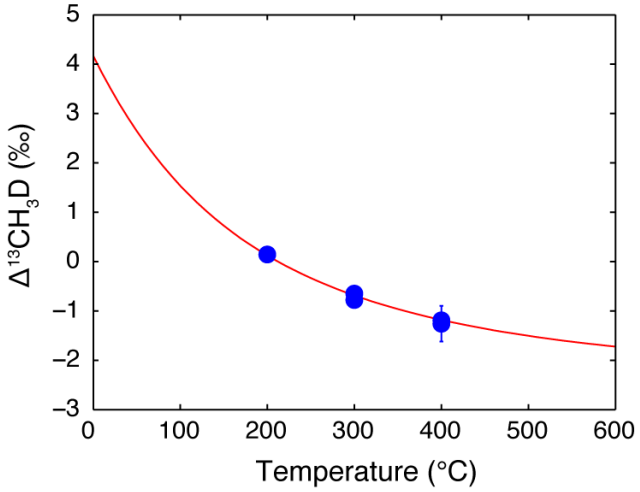

511

512 **Figure 7.** $\Delta^{13}CH_3D$ values for methane (working standard gas AL1) thermally equilibrated
513 between 200 and 400 °C. The values of $\Delta^{13}CH_3D$ are with respect to unheated AL1. The solid
514 line is a theoretical estimate, assuming $\Delta^{13}CH_3D$ value of reference AL1 is -2.29 ‰ against
515 stochastic distribution.

516

517

518

519

520

521

522

523 **Table 1.** Parameters for absorption lines selected for this study. Line position, strength, lower
524 state energy is from HITRAN database. Also shown is the temperature dependence of
525 absorption strength (dδ/dT).

	Frequency (cm^{-1})	Strength (cm/molecule)	Lower State Energy (cm^{-1})	γ_P ($cm^{-1}atm^{-1}$)		γ_{Dicke} (atm^{-1})	dδ/dT (‰/10mK)
				HITRAN	This study		
$^{12}CH_4$	1168.9466	4.45E-24	470.79	0.073	0.101	-11.4	0.08
$^{13}CH_4$	1330.9787	1.72E-24	1554.10	0.075	0.091	-9.8	0.25
$^{12}CH_3D$	1168.9099	1.01E-24	861.04	0.071	0.080	-12.4	0.14
$^{13}CH_3D$	1168.9812*	2.09E-25	58.87	0.081	0.126	-25.7	0.01

526

527 *In the HITRAN database, this line is split into 1168.98118 and 1168.98325 cm^{-1}.

528

529

530

531

532

533

534 **Table 2.** Isotopologue compositions for laboratory cylinder methane (AL1, AS1 and AS2). The
535 numbers in bold italic letters for AL1 indicate IRMS data, which is used to define $\delta^{13}C$ and δD
536 of the TILDAS instrument. 2σ represents 2×standard deviation for repeated measurements
537 (*n*, in parentheses).

538

	$\delta^{13}C_{PDB}$	2σ	δD_{SMOW}	2σ	$\Delta^{13}CH_3D^{*1}$	2σ	Temperature (°C)	2σ
Cylinder Methane								
AL1	***-34.5***	***0.5***	***-127***	***5***	2.29	0.10	212	-10/+11
AS1 (7)	-42.40	0.09	-161.07	0.07	2.79	0.17	167	-13/+14
AS2 (5)	-38.6	0.14	-133.5	0.04	2.49	0.08	193	-8/+7
House Natural Gas								
house gas (4)	-33.6	0.16	-140.7	0.16	3.00	0.54	151	-35/+44

539

540 *1: $\Delta^{13}CH_3D$ is with respect to stochastic (infinite-temperature) distribution.

541

Supporting Information for

"Measurement of Doubly-Substituted Methane Isotopologue, $^{13}CH_3D$, by Tunable Infrared Laser Direct Absorption Spectroscopy "

Shuhei Ono,, David T. Wang, Danielle S. Gruen*

Department of Earth, Atmospheric and Planetary Sciences, Massachusetts Institute of Technology, Cambridge, MA. sono@mit.edu

Barbara Sherwood-Lollar,

Department of Earth Sciences, University of Toronto, Toronto, ON, Canada

Mark S. Zahniser, Barry J. McManus, David D. Nelson

Center for Atmospheric and Environmental Chemistry, Aerodyne Research, Inc., Billerica, Massachusetts, USA

Supporting information includes:

1) Detailed protocol for synthesis of methane isotopologues.

2) Detailed definition and derivation of $\Delta^{13}CH_3D$, $\delta^{13}C$ and δD values, and theoretical estimate of the equilibrium constant (K) of isotope exchange reaction (1), and

3) Three figures (Figure S-1, S-2 and S-3) and one Table (Table S-1), which are mentioned in the main text.

1. Synthesis of Methane Isotopologues

The clumped methane isotopologue, $^{13}CH_3D$, was synthesized by the Grignard reaction. The Grignard reagent was synthesized from ^{13}C-iodomethane (1.2 mL, $^{13}CH_3I$, 99 atom % from Sigma Aldrich) and magnesium (0.5 g) in diethyl ether (9 mL) under helium flow, refluxing with a dry ice condenser, by the reaction:

$$^{13}CH_3I + Mg \rightarrow {}^{13}CH_3MgI \qquad (S1)$$

Deuterium oxide (0.7 mL, 99.96 atom %D, Cambridge Isotope Laboratory) was added dropwise to produce $^{13}CH_3D$:

$$^{13}CH_3MgI + D_2O \rightarrow {}^{13}CH_3D + Mg(OD)I \qquad (S2)$$

The product $^{13}CH_3D$ was adsorbed on a trap filled with activated charcoal immersed in liquid nitrogen. After the reaction, the carrier helium gas was pumped out and methane was desorbed from the trap. Mass-spectrometer analysis showed better than 99% purity. Similarly, CH_3D (with natural-abundance ^{13}C) was synthesized from iodomethane and D_2O.

D-depleted methane was synthesized from aluminum carbide (Al_4C_3, natural C isotope abundance) and D-depleted water (D content 2-3 ppm) via the reaction:

$$Al_4C_3 + 12H_2O \rightarrow 4Al(OH)_3 + 3CH_4 \qquad (S3)$$

Reaction (S3) readily proceeds at 80 °C. The product CH_4 was distilled at -110 °C. Gas chromatography analysis showed better than 99% purity with trace quantities of CO_2.

2. Definition and derivation of $\Delta^{13}CH_3D$, $\delta^{13}C$ and δD values, and theoretical estimate of the equilibrium constant (K)

The equilibrium constant (K) of the isotope exchange reaction among four isotopologues of methane:

$$^{13}CH_4 + {}^{12}CH_3D \leftrightarrow {}^{13}CH_3D + {}^{12}CH_4 \quad \text{(S4)}$$

was estimated by conventional theories of stable isotope fractionation.[1-3] Fundamental frequencies for $^{12}CH_4$ were taken from experimental values,[4] and the frequency shifts for three isotopologues ($^{13}CH_4$, $^{12}CH_3D$, and $^{13}CH_3D$) relative to $^{12}CH_4$ were estimated using molecular dynamics simulation at HF/6-31G* basis set.

The temperature dependence of the equilibrium constant can be approximated as:

$$\text{Ln}(K) = -5.256\text{x}10^{-1}\ T^{-1} + 1.0126*10^{3}\ \text{x}\ T^{-2} - 1.0579*10^{5}\text{x}T^{-3} \quad \text{(S5)}.$$

Previous study has shown that different levels of theory yield similar results.[2] Total partition function sums can also be calculated from spectroscopic data for each isotopologues.[5,6] Partition function sum of $^{12}CH_4$ and $^{13}CH_4$ from Fischer et al. (2003) and $^{12}CH_3D$ and $^{13}CH_3D$ from Laraia et al. (2011), however, yield K = 1.0009 at 296K, as opposed to 1.0057 derived by our model. The main reason could be due to the fundamental vibrational frequencies for $^{13}CH_3D$ used by Laraia et al. (2011).

Our definition of the $\Delta^{13}CH_3D$ value

$$\Delta^{13}\text{CH}_3\text{D} = \ln(K) = \ln\frac{\left[^{13}\text{CH}_3\text{D}\right]}{\left[^{12}\text{CH}_3\text{D}\right]} - \ln\frac{\left[^{13}\text{CH}_4\right]}{\left[^{12}\text{CH}_4\right]} \quad \text{(S6)}.$$

yields practically identical value to that defined by Stolper et al. (2014)[3] that referenced against "stochastic $^{13}CH_3D$ abundance", which is estimated from $^{13}CH_4$ and $^{12}CH_3D$. This is because,

$$\Delta^{13}\text{CH}_3\text{D} \equiv \ln\frac{\left[^{13}\text{CH}_3\text{D}\right]}{\left[^{12}\text{CH}_3\text{D}\right]} - \ln\frac{\left[^{13}\text{CH}_4\right]}{\left[^{12}\text{CH}_4\right]} = \ln\frac{\left[^{13}\text{CH}_3\text{D}\right]}{\left[^{12}\text{CH}_3\text{D}\right]}\frac{\left[^{12}\text{CH}_3\text{D}\right]}{\left[^{12}\text{CH}_4\right]} - \ln\frac{\left[^{13}\text{CH}_4\right]}{\left[^{12}\text{CH}_4\right]}\frac{\left[^{12}\text{CH}_3\text{D}\right]}{\left[^{12}\text{CH}_4\right]}$$

$$\simeq \ln\left(\frac{^{13}\text{CH}_3\text{D}}{^{12}\text{CH}_4}\right)_{\text{measured}} - \ln\left(\frac{^{13}\text{CH}_3\text{D}}{^{12}\text{CH}_4}\right)_{\text{stochastic}}$$

$$= ln\left(\frac{\left(\frac{^{13}\text{CH}_3\text{D}}{^{12}\text{CH}_4}\right)_{\text{measured}}}{\left(\frac{^{13}\text{CH}_3\text{D}}{^{12}\text{CH}_4}\right)_{\text{stochastic}}}\right)$$

$$\simeq \frac{\left(\frac{^{13}CH_3D}{^{12}CH_4}\right)_{measured}}{\left(\frac{^{13}CH_3D}{^{12}CH_4}\right)_{stochastic}} - 1 \qquad \text{(S7)}.$$

In practice, $\Delta^{13}CH_3D$ values are measured by comparing those of samples to laboratory working reference gas:

$$\Delta^{13}CH_3D_{sample} = \ln\frac{^{13}R_{sample}}{^{13}R_{reference}} - \ln\frac{^{13}r_{sample}}{^{13}r_{reference}} - \Delta^{13}CH_3D_{reference} \qquad \text{(S8)}$$

where, $^{13}R = {}^{13}CH_3D/{}^{12}CH_3D$ and $^{13}r = {}^{13}CH_4/{}^{12}CH_4$ of sample and working reference CH_4. Equation (S8) shows that there will be a constant offset to account for the non-zero $\Delta^{13}CH_3D$ value of the working reference gas. This value can be determined by calibrating against methane equilibrated at a range of known temperatures. For our reference gas (AL1) the $\Delta^{13}CH_3D_{reference}$ value was estimated to be -2.29 ±0.1 ‰ (Figure 7).

The apparent systematic relationship between δD and $\Delta^{13}CH_3D$ for bracketing experiments suggests unaccounted weak absorption line underneath $^{12}CH_3D$. If the hidden absorption line is due to $^{12}CH_4$, correction for this will be analogous to abundance sensitivity correction for isotope ratio-mass spectrometer due to tailing of the main isotopologue line onto minor isotopologue.[7] The absorption of the unaccounted line is estimated to be 0.01 % such that it may not be detected from the fit residual (Figure 2). The isotope delta scale will contract due to constant bias both for reference and sample isotopologue ratios. Following Ono et al. (2006)[7], when signal size for sample and reference is balanced, the correction is:

$$\delta D_{corrected} = (1+b)\ \delta D_{measured} \qquad \text{(S9)}$$

where the value b describes the relative contribution of $^{12}CH_4$ onto $^{12}CH_3D$ (b=0.002 is our best estimate), δD values in equation (S9) are with respect to working reference gas (AL1). The equation (S9) was used to correct δD values from which the ratio $^{12}CH_3D/{}^{12}CH_4$ is derived, and

then used to correct $\Delta^{13}CH_3D$ values. The magnitude of the correction is less than 0.8 ‰ when δD_{SMOW} is between -500‰ and 250 ‰.

Delta values in this study are reported with respect to PDB (Pee Dee Belemnite) and SMOW (Standard Mean Ocean Water). For isotopologue ratios, these are:

$$\delta^{13}C = \frac{\left({}^{13}CH_4/{}^{12}CH_4\right)_{sample}}{\left({}^{13}C/{}^{12}C\right)_{PDB}} - 1 \quad , \qquad \text{(S10)}$$

and

$$\delta D = \frac{\left({}^{12}CH_3D/{}^{12}CH_4\right)_{sample}}{4\cdot(D/H)_{SMOW}} - 1 \qquad \text{(S11)}$$

Factor four in equation (S11) reflects four H atoms in CH_4. These delta values are derived by comparison with laboratory reference gas (AL1), which has $\delta^{13}C$ and δD of -34.5 ± 0.5‰ and -127 ± 5‰ (2σ), respectively, as measured by GC-IRMS at the University of Toronto (Table 2). These uncertainties include analytical precision and overall accuracy.

Reference in Supporting Information

(1) Schauble, E. A. *Reviews in Mineralogy* **2004**, *55*, 65--111.
(2) Ma, Q.; Wu, S.; Tang, Y. *Geochimica et Cosmochimica Acta* **2008**, *72*, 5446--5456.
(3) Stolper, D.; Sessions, A.; Ferreira, A.; Santos Neto, E.; Schimmelmann, A.; Shusta, S.; Valentine, D.; Eiler, J. *Geochimica et Cosmochimica Acta* **2014**, *126*, 169--191.
(4) Shimanouchi. *Tables of molecular vibrational frequencies Consolidated Volume I*; National Bureau of Standards, 1972, p 1--160.
(5) Laraia, A. L.; Gamache, R. R.; Lamouroux, J.; Gordon, I. E.; Rothman, L. S. *Icarus* **2011**, *215*, 391-400.
(6) Fischer, J.; Gamache, R. R.; Goldman, A.; Rothman, L. S.; Perrin, A. *Journal of Quantitative Spectroscopy and Radiative Transfer*, *82*, 401-412.
(7) Ono, S.; Wing, B.; Rumble, D.; Farquhar, J. *Chemical Geology* **2006**, *225*, 30-39.

3. Supporting figures and a table

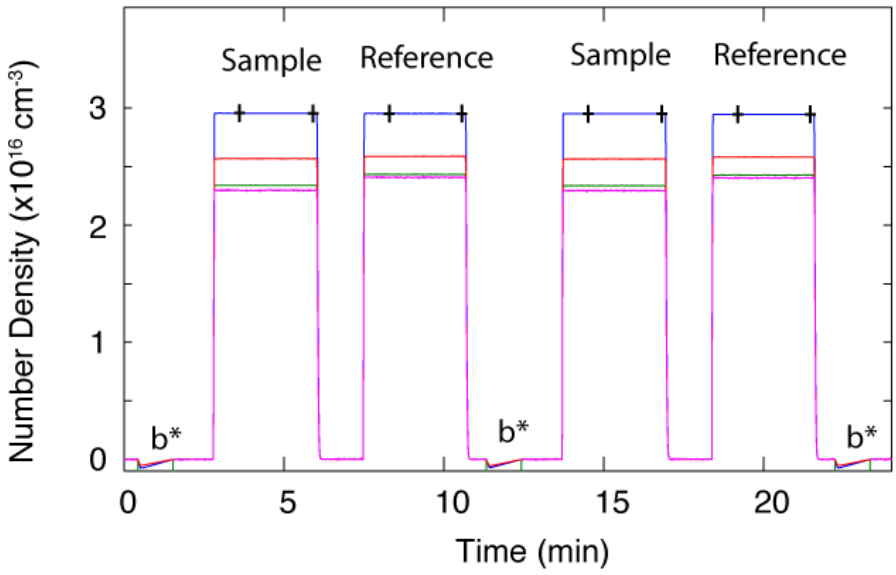

Figure S-1. Example of measurement cycles. Each line shows the number density as a function of time (blue $^{13}CH_4$, red, $^{12}CH_4$, green $^{12}CH_3D$, and purple, $^{13}CH_3D$). Signals were averaged between two crosses. Each measurement cycle consists of baseline calibration (marked as b*, 60 seconds), and measurements of sample and reference (190 seconds each). Number density for minor isotopologues was divided by its fractional abundance used by HITRAN database.

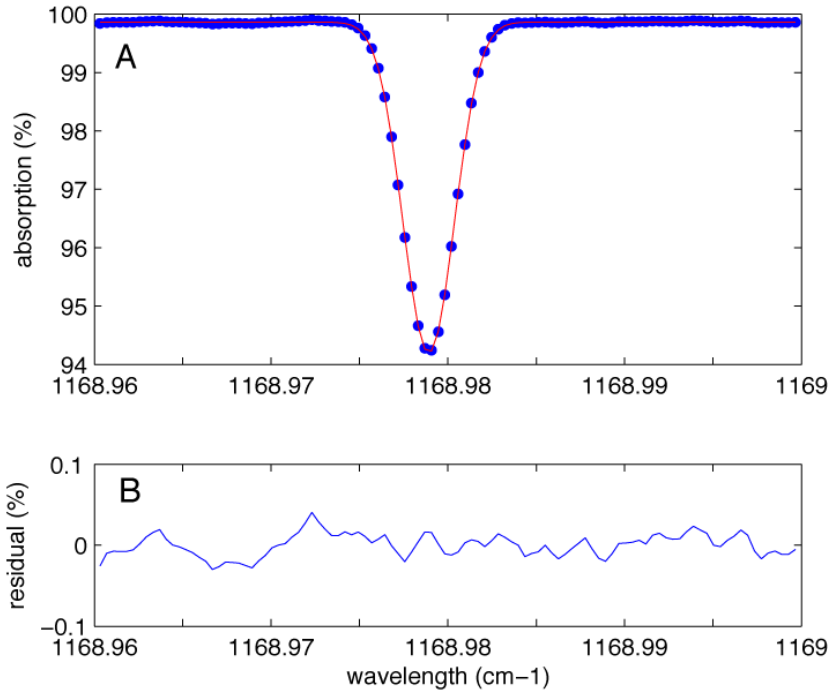

Figure S-2. TILDAS spectrum for pure $^{13}CH_3D$ (measurements in blue points, and fit in red line) (A), and residual for spectrum fitting. Best fit was obtained with single absorption line with Doppler line width of 0.001688 cm^{-1} (0.001696 cm-1 is theoretical value). Cell pressure is less than 1 mbar.

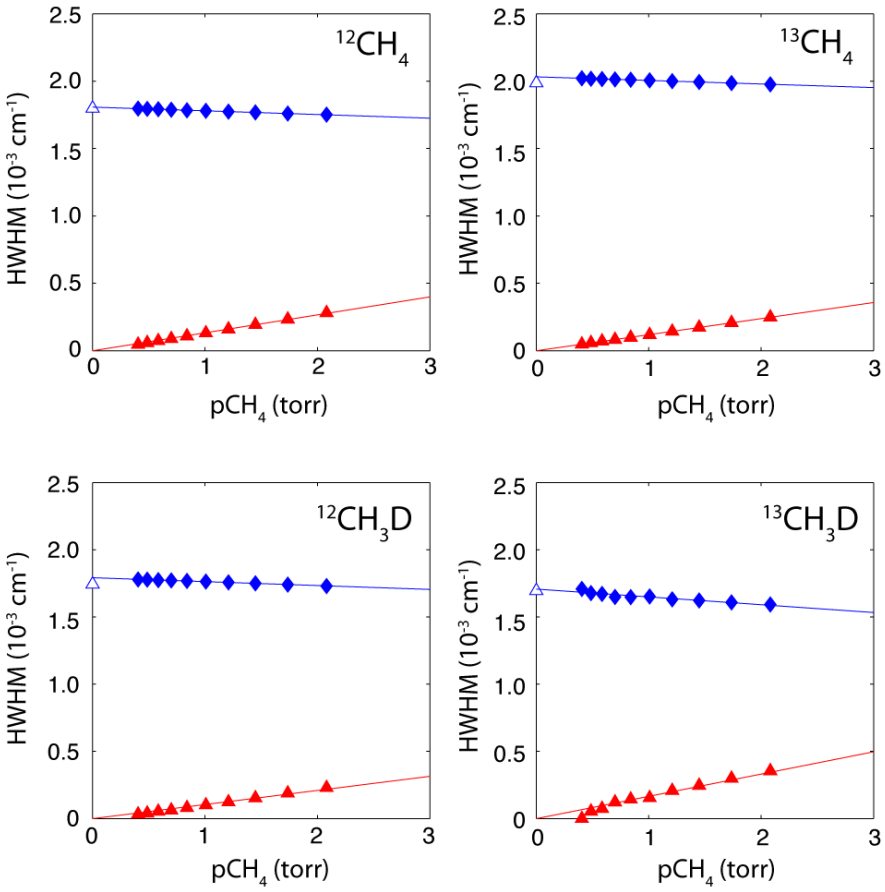

Figure S-3. Line width parameters derived from least square fit of absorption lines between 0.4 to 2.1 torr CH_4. The spectrum was deconvoluted to Gaussian (filled diamond) and Lorentzian components (solid triangle). Also shown is the expected Doppler line width (open triangle).

Table S-1. Results for heated methane experiments.

CH_4 source	T (°C)	Duration (days)	$\delta^{13}C_{PDB}$	2SEM*[1]	δD_{SMOW}*[2]	2SEM*[1]	$\Delta^{13}CH_3D$*[2]	2SEM*[1]
Time Series Experiment								
AL2-D3	initial		-39.01	0.02	-133.69	0.02	36.77	0.20
AL2-D3	initial		-39.01	0.02	-133.72	0.05	36.97	0.20
AL2-D3	200	5.0	-38.93	0.01	-152.45	0.03	3.48	0.10
AL2-D3	200	8.2	-38.86	0.03	-155.31	0.02	0.46	0.28
AL2-D3	200	13.0	-38.90	0.01	-155.84	0.05	0.21	0.20
AL2-D3	200	17.0	-38.87	0.02	-154.83	0.03	0.12	0.15
AL2-D3	200	19.0	-38.92	0.02	-157.10	0.03	0.08	0.15
Thermal Equilibrium Experiment								
AL1	200	11	-34.29	0.01	-146.83	0.01	0.14	0.09
AL1	200	20	-34.58	0.04	-143.70	0.03	0.14	0.12
AL1	300	12	-34.51	0.01	-147.64	0.02	-0.65	0.07
AL1	300	20	-34.63	0.02	-153.94	0.03	-0.78	0.12
AL1	400	2	-34.96	0.02	-143.82	0.08	-1.26	0.36
AL1	400	6	-34.93	0.02	-142.92	0.04	-1.19	0.14
δD Bracketing Experiment								
AL1-D2	initial		-34.53	0.02	36.75	0.04	-0.95	0.18
AL1-D2	initial		-34.47	0.03	36.96	0.01	-0.52	0.15
AL1-D2	400	1	-34.51	0.02	35.23	0.07	-0.63	0.18
AL1-D2	400	16	-34.50	0.03	28.75	0.04	-0.20	0.27
AL1-D3	initial		-34.53	0.02	272.88	0.03	-1.34	0.20
AL1-D3	initial		-34.51	0.01	273.36	0.03	-0.88	0.16
AL1-D3	initial		-34.50	0.02	273.42	0.05	-1.21	0.15
AL1-D3	400	1	-34.53	0.03	105.82	0.05	-0.68	0.30
AL1-D3	400	17	-34.97	0.02	133.59	0.03	-1.03	0.13
AL1-D3	400	9	-34.50	0.02	81.39	0.03	-1.02	0.09
AL1-D5	initial		-40.31	0.03	-339.65	0.04	5.19	0.18
AL1-D5	400	14	-38.99	0.02	-250.33	0.03	-0.86	0.10
AL2-D4	initial		-50.48	0.02	-628.62	0.05	44.22	0.23
AL2-D4	400	2	-45.50	0.01	-385.07	0.03	-0.75	0.13
AL2-D4	400	4	-45.64	0.24	-378.91	0.26	-0.79	0.35

*1: Standard error of the mean (SEM) is estimated from standard deviation from 10 to 14 measurement cycles.

*2: Reported δD and $\Delta^{13}CH_3D$ value includes scale expansion factor of 1.002 for δD. $\Delta^{13}CH_3D$ value is with respect to reference gas AL1 (i.e., subtraction of 2.29 ‰ yields the $\Delta^{13}CH_3D$ value with respect to stochastic distribution).